A four-chip parallel IGBT module based on the latest generation technology used in Photovoltaic Centralized Inverter

Zhang Tao[1], Wang Xuanxuan[1], Rong Rui[1], Cao Shuai[1], Miao Shuo[1], Chen Guokang[1]

[1] Macmic science & technology Co.,Ltd.,China

tzhang@macmicst.com

The Power Point Presentation will be available after the conference.

Abstract

This paper introduces the application of four-chip parallel IGBT module using the 7th generation of chip technology in photovoltaic centralized inverter. There are not many products worldwide that can achieve four chip parallel connection. Parallel connection of four chips puts forward high requirements for chip consistency. In addition, the power loss of each part is accurately calculated, and the total loss of our module is more than 5% lower than other competitive products on the market. This product is able to support the working temperature of 175℃, and has high reliability in special application scenarios.

1 Introduction

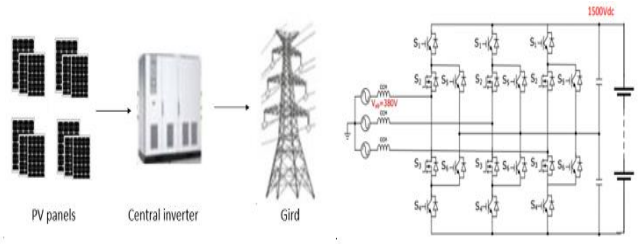

Fig. 1. Principle of photovoltaic inverter

The power requirements of photovoltaic inverters are increasing as the market changes. The 7th chip has increased its current density on the original basis, resulting in an advancement in power without changing the chip size.

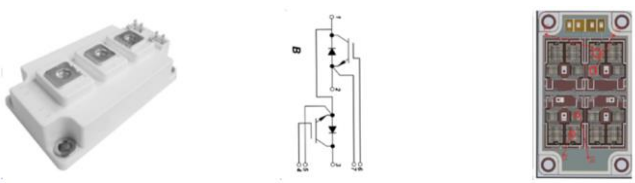

Fig. 2. Product outline drawings and layout drawings

The two figures on the left show the package and internal topology of MacMic's four-chip parallel module. The picture on the far right shows how to complete the layout of four chips in one module.

Chapter 2 shows the main features of the IGBT module. Chapter 3 introduces the simulation results of our products in different application scenarios. Chapter 4 describes our ability to maintain high reliability at 175 °C temperatures and in extreme environments. Chapter 5 gives the summary.

2 Production information

Item	Value
Collector Emitter Voltage	1200V
Implemented Collector current	800A
Operating junction temperature	175℃
Size	108×62×30.5mm
Weight	300g
Vcesat	1.5V
Gate Charge	3.5uC
Turn on loss(150℃)	25.4mJ
Turn off loss(150℃)	121mJ

Table. 1. Main features of GD module

The features of our product have certain advantages over other products on the market.

2.1 Double pulse test

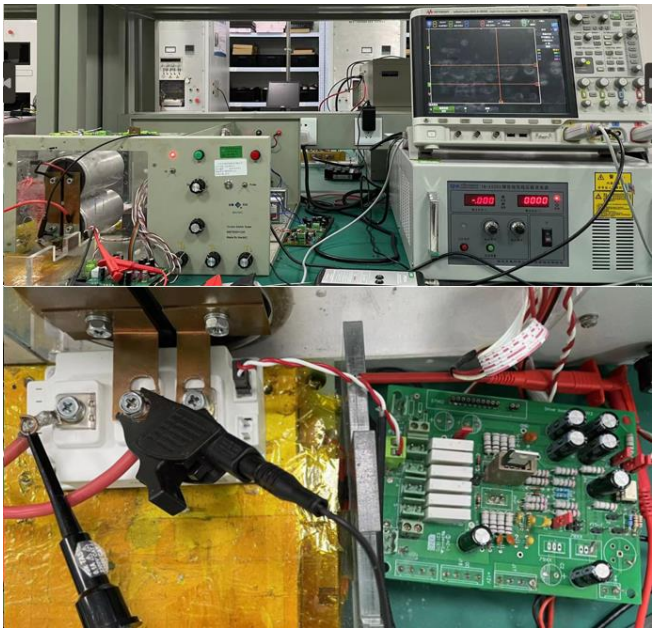

Fig. 3. Double pulse testing machine

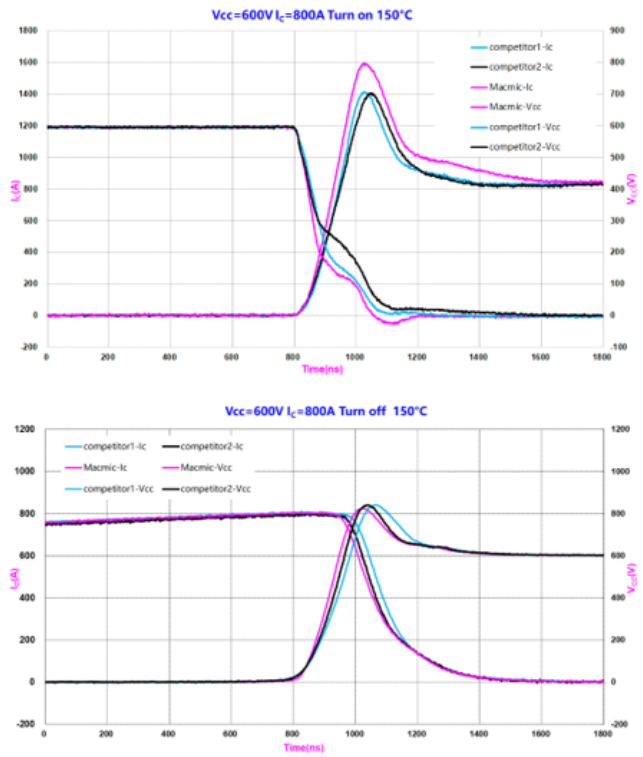

Fig. 4. Test waveform

Under high temperature conditions, the switching speed of Macmic is faster than that of competitive products, so our products have better opening loss. Our module has the right switching speed and good loss performance during the whole machine operation.

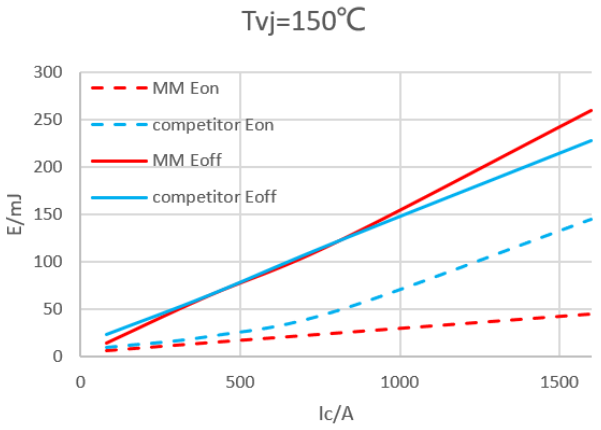

Fig. 5. Loss contrast curve

This fig. shows that the opening loss of Macmic is better than that of competitors when the rated current is less than 800A.However our loss is larger when the rated current is exceeded. And it gets worse as the current increases. Our modules have a lower turn-off loss than competing products. This phenomenon becomes more and more obvious as the current increases. In applications such as photovoltaics with a large proportion of turn-off losses, the advantages of our modules will be quite obvious.

3 Simulation Result

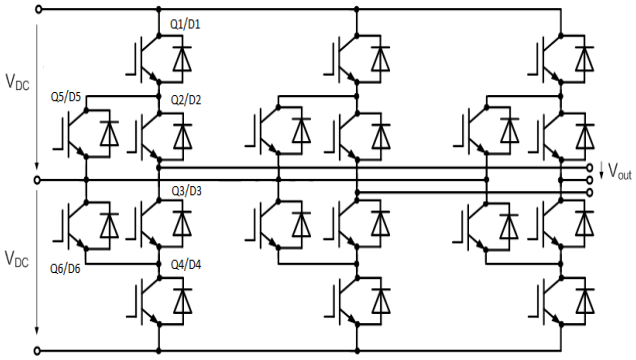

Fig. 6. Circuit topology diagram

ANPC is the actual circuit topology used. Customers may use modules in parallel on the basis of three-phase and three-level according to the difference in power.

3.1 Loss calculation formula

3.1.1 Conduction loss

A functional simulation is immensely helpful for setting up the power loss equations. Such a simulation as in Figure 6 shows the modulation (control) signal, the electrical angle θ, phase current lagging by the phase angle φ, the forward current through Q1, reverse current through D1 (really the intrinsic diode of Q1 if it is a FET), and the gate control signal for Q1.

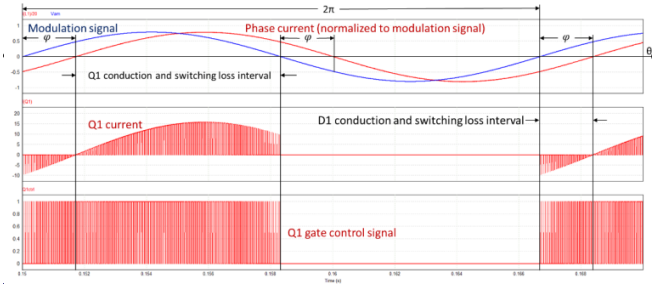

Fig. 7. Phase angle, conduction, and switching loss intervals for 3L-ANPC PWM1

One complete AC line cycle spans 2π radians of θ, but Q1 conducts forward (positive) current only during half a line cycle.

$$P_{CQ1} = \frac{\mathrm{m}}{2\pi}\left[2I_{pk}^2 R_{ds}(1-\cos\varphi)^2 + 3I_{pk}V_0[-\varphi\cos\varphi + \sin\varphi]\right]$$

In this equation, m is the modulation index and I_{pk} is the peak current in a single FET since we are solving for the per FET power loss. R_{ds} is the FET $R_{DS(ON)}$, and V_0 is the knee voltage of the FET, which is always zero for UnitedSiC FETs, but including it allows the equations to

be applied to bipolar type devices such as IGBTs with output characteristic modelled as a straight line with an offset.

3.1.2 Switching loss

Switching loss can be modelled as a second-order polynomial, with data taken from datasheet graphs, and adjusted for temperature. For example, the turn-on switching energy versus drain current I_d is modelled as in the equation below where a_w, b_w, and c_w are polynomial coefficients.

$$E_{on} = a_w \cdot I_d^2 + b_w \cdot I_d + c_w$$

The coefficients are used in an integral to calculate switching loss, similar to conduction loss.

$$P_{swQ1} = \left[\frac{1}{2\pi}\int_{\varphi}^{\pi}\left[a_w(I_{pk}\sin(\theta-\varphi))^2 + b_w I_{pk}\sin(\theta-\varphi) + c_w\right]d\theta\right]\frac{V_{DC}/2}{V_{ref}}f_{sw}$$

It is reasonable to assume that the switching loss scales with the total DC link voltage, which is V_{DC} in the top equation. Note that only half the DC link voltage is switched in a three-level inverter, so V_{DC} is divided by 2. The voltage used to characterize the switching energies in the datasheet is V_{ref}, and f_{sw} is the switching frequency.

3.2 PV inverter scenario

Vdc(V)	1500
Vout(V)	900
Iout(A)	565
Fout(Hz)	50
Fsw(Hz)	3600
Rg_on(Ω)	2
Rg_off(Ω)	2.7
Modulation Algorithm	PWM
Modulation Index	1
cosφ	1

Table. 2. Simulation input condition

We visited a lot of clients. They introduced to us the application conditions of the product in the actual use process, and we used these conditions to do some simulation analysis, so as to make our product more successful.

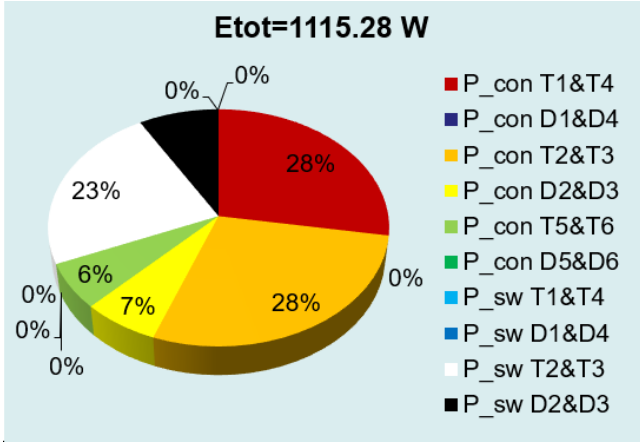

Fig. 7. PWM 1 modulation loss distribution

As we can see from this picture, the conduction loss of IGBT accounts for the majority. It is necessary for us to consider its low Vcesat when designing the chip.

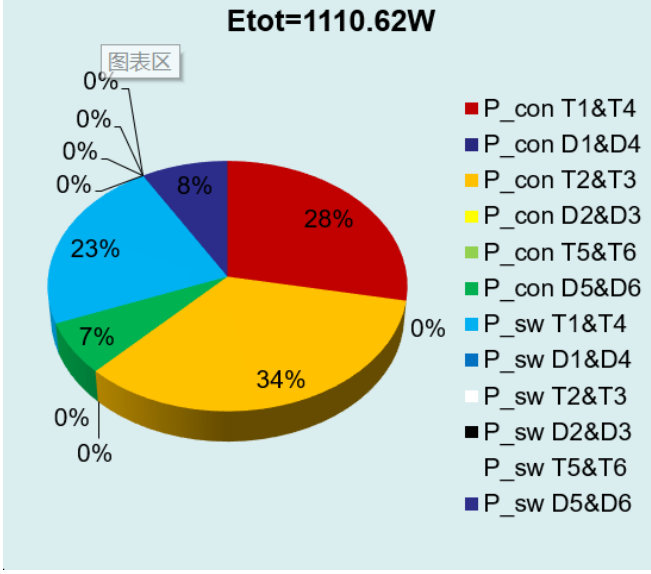

Fig. 8. PWM 2 modulation loss distribution

In the PWM2 modulation mode, the conduction loss is also our most concerned characteristic.

3.3 Energy storage scenario

Vdc(V)	1500
Vout(V)	900
Iout(A)	565
Fout(Hz)	50
Fsw(Hz)	3600
Rg_on(Ω)	2
Rg_off(Ω)	2.7
Modulation Algorithm	PWM
Modulation Index	1
cosφ	-1

Table. 3. Simulation input condition

The difference between the energy storage response and the PV application is that its power factor is -1.

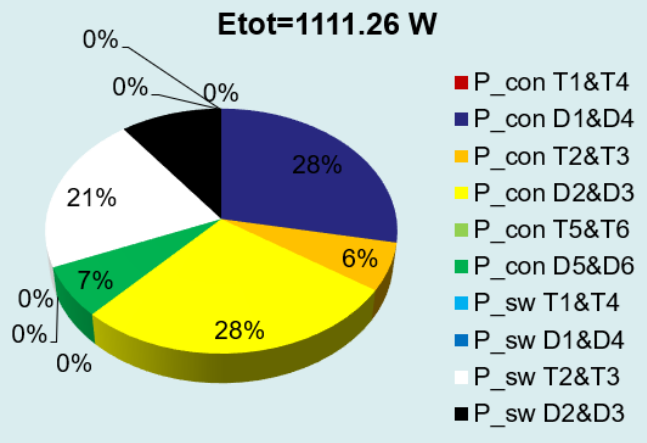

Fig. 9. PWM 1 modulation loss distribution

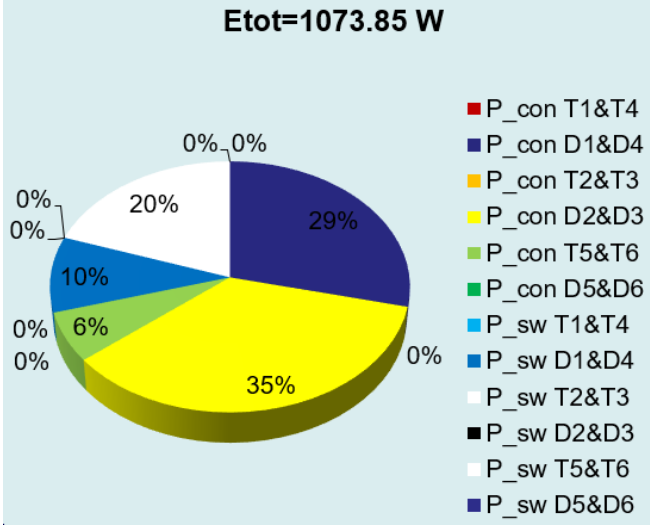

Fig. 10. PWM 1 modulation loss distribution

These two graphs show the distribution of losses under energy storage applications. In this application, the conduction loss of FRD plays a major role. This means that we need the FRD to have a low VF.According to the customer's specific application conditions, different modulation methods will bring different loss results. We should consider both photovoltaic application scenarios and energy storage application scenarios when designing products.

4 Experimental Result

4.1 High Operating junction temperature

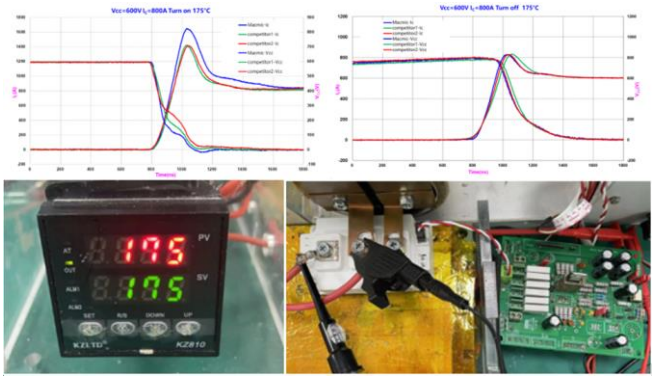

Fig. 11. 175℃ temperature waveform

When heated to the ambient temperature of 175℃, the module has the ability to work normally, and the electrical performance will not change due to the high temperature, so our product can work normally at 175℃ junction temperature for a period of time.

4.2 High Reliability

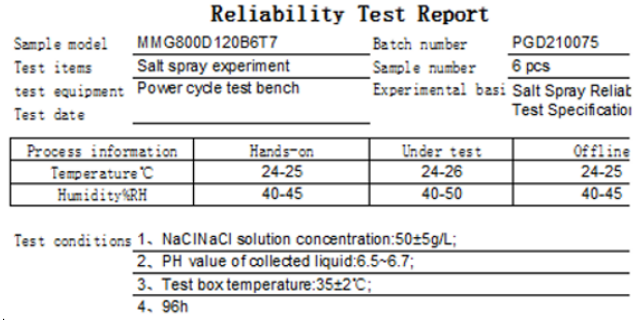

Reliability Test Report

Sample model	MMG800D120B6T7	Batch number	PGD210075
Test items	Salt spray experiment	Sample number	6 pcs
test equipment	Power cycle test bench	Experimental basi	Salt Spray Reliat Test Specificatio
Test date			

Process information	Hands-on	Under test	Offline
Temperature℃	24-25	24-26	24-25
Humidity%RH	40-45	40-50	40-45

Test conditions 1、NaCINaCl solution concentration:50±5g/L;
2、PH value of collected liquid:6.5~6.7;
3、Test box temperature:35±2℃;
4、96h

Fig. 12. Salt spray test

Salt spray test is a kind of environmental test which mainly uses artificial simulated salt spray environmental conditions created by salt spray test equipment to assess the corrosion resistance of products or metal materials. To verify whether the metal parts on the product will corrode when exposed to the atmosphere or other environment. The product can be placed in the use environment for a long enough time, such as a product lifecycle. Salt spray testing is an accelerated corrosion resistance evaluation method for artificial atmospheres.

5 Conclusion

References The four-chip parallel module enables the existing package to have greater current capacity, allowing the output power of the inverter to be increased under the same package size. We can reduce the cost by simplifying the inverter system. For ultra-high power devices, we can reduce the number of modules in parallel, so that the current can be evenly distributed to each module. The 7th generation IGBT chip technology provides high reliability guarantee while ensuring performance optimization. The successful development of 800A module is a major breakthrough.

6 References

[1] Thomas Geinzer, et al, Value creationdeveloping efficient 750V IGBT and emittercontrolled diode for automotive applications,PCIM Europe 2015, 19 – 21 May 2015,Nuremberg, Germany

[2] Jonathan Dodge, 3L-ANPC vs. 3L-NPC Inverters, Application Note: UnitedSiC_AN0023, February 2020

[3] Andre Christmann, David Levett, Design of a Power Module for Automotive and CAV Traction Drives, Bodo’s Power